Comparison of CP-OFDM and OFDM/OQAM in Doubly Dispersive Channels

Jinfeng Du, and Svante Signell, Senior Member, IEEE
Department of Electronic, Computer, and Software Systems
KTH - Royal Institute of Technology, Stockholm, Sweden
{jinfeng, srs}@kth.se

Abstract

In this paper we compare the performance of cyclic prefix based OFDM (CP-OFDM) systems and OFDM/offset QAM (OFDM/OQAM) systems in doubly dispersive channels, by investigating the signal reconstruction perfectness, time and frequency dispersion robustness, and sensitivity to frequency offset. Both analysis and simulation results show that various parameter adaptations can be made with respect to the channel state information to improve the system performance.

1. Introduction

Multicarrier communication technologies are promising candidates to realize high data rate transmission in Beyond 3G and further wireless systems where the channel is mostly doubly dispersive. In the classic orthogonal frequency division multiplexing (OFDM) transceiver the IFFT/FFT block are used together with a cyclic prefix to partition the frequency selective channel into a large number of parallel flat fading channels as long as the time spread does not exceed the length of the cyclic prefix. Such a cyclic prefix, however, fails to combat ICI caused by frequency dispersion and costs loss of energy and spectral efficiency.

OFDM/OQAM systems [1] which can achieve smaller ISI/ICI without using the cyclic prefix compared to classic OFDM systems utilize well designed pulse shapes that satisfy the perfect reconstruction conditions [2, 3]. Performance evaluation of OFDM/OQAM has already illustrated promising advantage [4, 6] and it has already been introduced in the TIA's Digital Radio Technical Standards [5] and been considered in WRAN (IEEE 802.22) [6], where the robustness of OFDM/OQAM to frequency dispersion is not taken into account. Equalization has to be introduced in OFDM/OQAM systems in presence of a dispersive channel and therefore either increases the complexity or degrades its advantage against CP-OFDM. The purpose of this paper is to take a close look at the integration issue of CP-OFDM and OFDM/OQAM systems and investigate how the system parameters affect the performance.

The rest of this paper is organized as follows. Section 2 presents the system model and several prototype functions. The effect of time and frequency dispersion is analyzed in Section 3. Simulation results are presented in Section 4 and conclusions are drawn in Section 5.

This work was supported in part by Wireless@KTH.

2. System Model and Pulse Shapes

2.1. System Model

The transmitted signal in CP-OFDM and OFDM/OQAM systems can be written in the following analytic form

$$s(t) = \sum_{n=-\infty}^{+\infty} \sum_{m=0}^{N-1} a_{m,n} g_{m,n}(t), \tag{1}$$

where $a_{m,n} (n \in \mathbb{Z}, m = 0, 1, ..., N-1)$ denotes the symbol conveyed by the sub-carrier of index m during the symbol time of index n, and $g_{m,n}(t)$ represents the synthesis basis which is obtained by time-frequency translation of the prototype function $g(t)$. In CP-OFDM systems

$$g_{m,n}(t) = e^{j2\pi mFt} g(t - n(T + T_{cp})), \;\; TF = 1 \tag{2}$$

where T and F are the symbol duration and inter-carrier frequency spacing respectively, $a_{m,n}$ are complex valued symbols and $g(t)$ is the rectangular function

$$g(t) = \begin{cases} \frac{1}{\sqrt{T+T_{cp}}}, & -T_{cp} \le t \le T \\ 0, & \text{elsewhere} \end{cases}$$

In OFDM/OQAM systems

$$g_{m,n}(t) = e^{j(m+n)\pi/2} e^{j2\pi m\nu_0 t} g(t - n\tau_0), \;\; \nu_0\tau_0 = 1/2 \tag{3}$$

where $a_{m,n}$ are real valued symbols with symbol duration τ_0 and inter-carrier spacing ν_0 respectively. The prototype

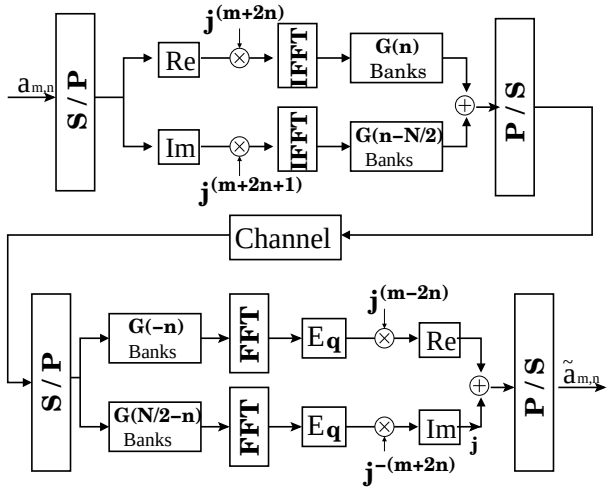

Figure 1. OFDM/OQAM system diagram.

pulse shape $g(t)$ is supposed to be a real and even function which can satisfy the perfect reconstruction condition in the absence of a channel. When there is a channel present, equalization has to be introduced to maintain the orthogonality between different bases.

To make a fair comparison, the sampling frequency F_s is assumed to be identical in CP-OFDM and OFDM/OQAM systems. This also makes it easier to switch between these two systems. One can either set $\nu_0 = F$ and shorten symbol duration [7], or set $\tau_0 = T$ and double the number of subcarriers [8]. We use the former approach.

An efficient implementation method by direct discretization of the continuous time model has been derived in [9] and implemented in the Matlab/Octave Simulation Workbench for Software Defined Radio [10]. The system diagram is shown in Fig. 1. Note that pulse shaping is realized by cooperation of the IFFT/FFT block and the bank of component filters. Using only the bank of component filters cannot achieve perfect or near perfect reconstruction. The equalization block is exactly the same as in the classic CP-OFDM system (one-tap zero-forcing frequency domain equalizer (FDE)) to reduce complexity. This will largely degrade the system performance in certain scenarios [11], as we will see later.

It is not a good idea to introduce cyclic prefix in the OFDM/OQAM system. If it is introduced near the channel (i.e., after the bank of component filters), removing the cyclic prefix at the receiver before passing through component filters will introduce discontinuity in the pulse shaping and therefore seriously degrade the orthogonality between the transmit and receive pulse shapes, which will consequently cause extra distortion. If cyclic prefix is introduced near IFFT/FFT blocks (i.e, the same as in OFDM systems), it will be no longer *cyclic* after passing through the bank of component filters and therefore cannot help to diagonalise the multipath channel. On the other hand, however, it will increase the symbol duration and therefore loosen the TFL requirement for pulse shape design.

2.2. Prototype Functions

Three kind of prototype functions will be considered in the following analysis, namely the Extended Gaussian function (EGF) [12], the half cosine function

$$g(t) = \begin{cases} \frac{1}{\sqrt{\tau_0}} \cos \frac{\pi t}{2\tau_0}, & |t| \le \tau_0 \\ 0, & \text{elsewhere} \end{cases} \tag{4}$$

and its frequency dual

$$G(f) = \begin{cases} \frac{1}{\sqrt{\nu_0}} \cos \frac{\pi f}{2\nu_0}, & |f| \le \nu_0 \\ 0, & \text{elsewhere} \end{cases} \tag{5}$$

Actually (5) is a special case of the square-root raised-cosine pulse in the frequency domain with roll-off factor $\rho = 1$, therefore it will be referred as RRC from now on.

3. Time and Frequency Dispersion Immunity Analysis

Let $T_s = 1/F_s$ be the sampling interval and assume that the time and frequency dispersive channel has Q resolvable paths $h_q,\ q = 0, 1, 2, ..., Q-1$, each with time spread $\epsilon_q T_s$, Doppler shift $f_d(q)$, power amplitude α_q and random phase shift φ_q. $\tau_d = \max_{i,j} |\epsilon_i - \epsilon_j| * T_s$ is defined as the delay spread and $B_D = \max_{i,j} |f_d(i) - f_d(j)|$ as the Doppler spread. The frequency response of the of the k_{th} sub-channel (regardless of the noise) can be written as

$$\begin{aligned} H_k(f) &= \sum_{q=0}^{Q-1} \alpha_q e^{j\varphi_q} e^{-j2\pi\epsilon_q(f+kF+f_d(q))/F_s} \\ &= \sum_{q=0}^{Q-1} \alpha_q e^{j\varphi_q} e^{-j2\pi(k+\frac{f+f_d(q)}{F})\frac{\epsilon_q}{N}} \end{aligned} \tag{6}$$

where $F = F_s/N$ is the bandwidth of each sub-channel. If we want to decrease the distortion from the time spread we have to increase the FFT size N since a sufficiently small value of $\frac{\tau_d}{NT_s}$ will make the multipath effects trivial and therefore insure a flat fading channel where the one-tap equalizer is sufficient. On the other hand, an increased N will decrease the sub-channel bandwidth $F = \frac{F_s}{N}$ accordingly, which in turn increases the sensitivity to Doppler spread ($\frac{B_D}{F}$ increases). Therefore a trade-off between small equalization loss and small Doppler spread distortion has to be taken into consideration in adaptation of system parameters with respect to different channel conditions. When the

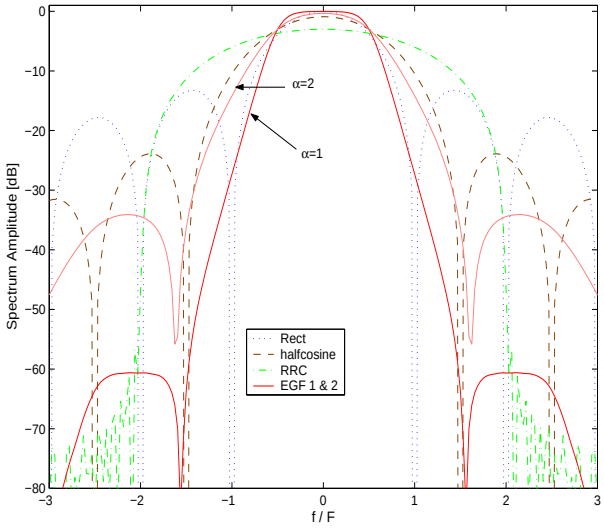

Figure 2. Pulse shape spectrum.

distortion caused by Doppler shift is dominating (compared to time dispersion and noise), using a smaller FFT size will increase the overall performance, and vice versa.

The equivalent channel transfer function between the k_{th} sub-channel at the transmitter and the l_{th} sub-channel at the receiver can be written as

$$\tilde{H}_{l,k}(f) \quad = G(f)H_{l-k}(f)G^*(f) = |G(f)|^2 H_{l-k}(f) \quad (7)$$

where $G(f)$ is the Fourier transform of $g(t)$. Suppose the strongest path h_0 is perfectly synchronized, i.e. $\epsilon_0 = 0$ and $f_d(0) = 0$, the pulse shape whose overall power spectrum $|G(f)|^2$ has a narrow main lope with flat top and fast decay side lope will be optimal to minimize the interference from neighboring sub-channels. Unfortunately it is not realistic as such a band limited function will have a large spread in time domain, which means a considerably long filter or large truncation error. Fig. 2 shows the spectrum amplitude $|G(f)|$ for the rectangular function, the half cosine function and its dual RRC, and EGF functions with factor $\alpha = 1$ and $\alpha = 2$ in the Gaussian function $g_\alpha(t) = (2\alpha)^{1/4} e^{-\pi\alpha t^2}$, $\alpha > 0$.

For different channels, the optimal pulse shape is normally different. A widely used parameter to measure the time frequency localization of the pulse shape is the Heisenberg parameter [2] $\xi = \frac{1}{4\pi\Delta t\Delta f} \leq 1$ with its maximum achieved by the Gaussian function. Δt is the mass moment of inertia of the prototype function in time and Δf in frequency, which indicates how the energy (mass) of the prototype function spreads over the time and frequency plane.

$$\begin{cases} (\Delta t)^2 & = \int_{\mathbb{R}} t^2 |g(t)|^2 dt \\ (\Delta f)^2 & = \int_{\mathbb{R}} f^2 |G(f)|^2 df \end{cases} \quad (8)$$

Here $g(t)$ is assumed to be origin-centered with unity energy [3] for simple expressions.

4. Numerical Results

Two kinds of channels are used in the following simulation, with the channel parameters in Table 1. In both of the two channels the delay spread $\tau_d = 14T_s$ and the Doppler spread $B_D = 10^{-5}F_s$. For a carrier frequency $f_c = 2GHz$ and sampling frequency $F_s = 7.68MHz$, the normalized Doppler spread $B_D/F_s = 10^{-5}$ is equivalent to a moving speed of 41.5km/h.

Table 1. Channel parameters

A	paths	1	2	3	4	5	6
	Delay [T_s]	0	2	4	7	11	14
	Power [dB]	0	-7	-15	-22	-24	-19
	Doppler	Doppler spread $B_D/F_s = 10^{-5}$					
B	paths	1	2	3	4	5	6
	Delay [T_s]	-3	0	2	4	7	11
	Power [dB]	-6	0	-7	-22	-16	-20
	Doppler	Doppler spread $B_D/F_s = 10^{-5}$					

4.1. TFL and Orthogonality

Table 2 lists the Heisenberg parameter ξ and orthogonality parameter $\gamma_I^2 = \sum |\tilde{a}_{m,n} - a_{m,n}|^2$ for different pulse shapes, where $a_{m,n}$ is the transmitted symbol and $\tilde{a}_{m,n}$ is the reconstructed signal, as shown in Fig. 1. γ_I^2 is actually the distortion power introduced by non-perfect reconstruction through an ideal channel. The OFDM system is used for the rectangular pulse and OFDM/OQAM is used for others with $\frac{\tau_0}{T} = \frac{1}{2}$ and $\frac{\nu_0}{F} = 1$. 12 time and frequency intervals are used and each interval contains 32 samples.

Table 2. TFL (ξ) and orthogonality (γ_I^2)

pulse	OFDM rect*	halfcosine	RRC	EGF $\alpha = 1$	EGF $\alpha = 2$
TFL ξ	0.178	0.895	0.888	0.874	0.977
γ_I^2 [dB]	-314	-309	-69	-96	-178

* for rectangular pulse, $(\Delta f)^2 = \int f^2 \text{sinc}^2(wf)df = \infty$ and therefore $\xi = 0$ in theory.

CP-OFDM and OFDM/OQAM with the half cosine function can achieve perfect reconstruction in the absence of a channel as the level of distortion power reaches the resolution limit of a double precision number ($\approx 10^{-15}$). For

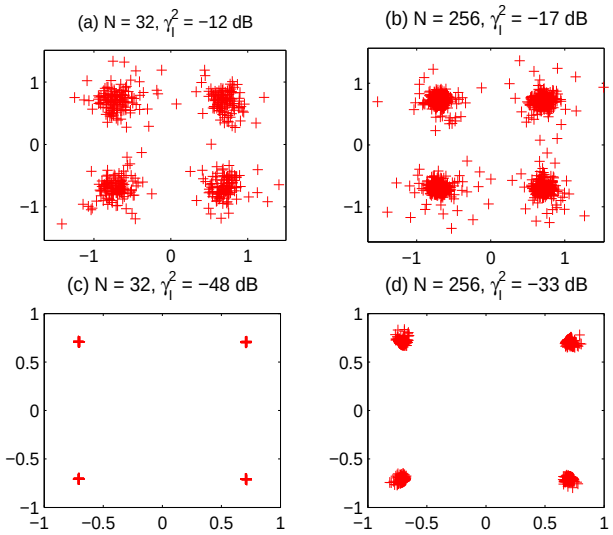

Figure 3. CP-OFDM signal reconstruction with channel B with $B_D = 0$ used in (a), (b) and channel A used in (c), (d).

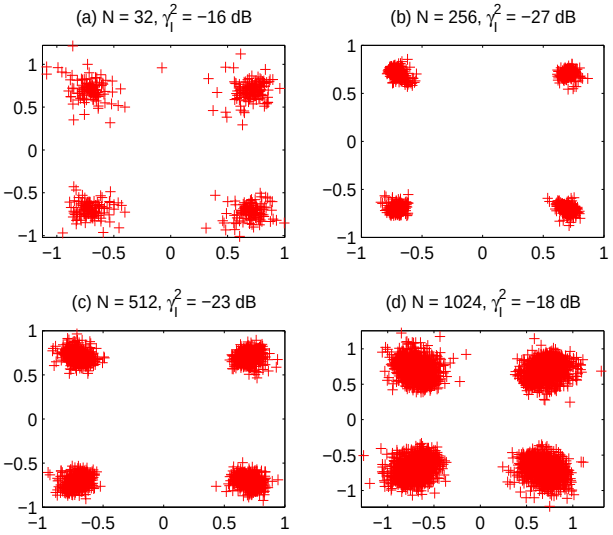

Figure 4. OFDM/OQAM signal reconstruction with EGF ($\alpha = 2$) through channel A.

other pulses, the introduced distortion power is also limited. Note that EGF with $\alpha = 2$ achieves the best TFL among pulse shapes and better reconstruction than EGF with $\alpha = 1$, we will therefore use $\alpha = 2$ for EGF in the following.

4.2. Signal Reconstruction in Doubly Dispersive Channel

In this section we present various simulation results for signal reconstruction in doubly dispersive channels. Noise is not introduced so that all the distortion comes either from time spread or frequency spread. A cyclic prefix with length $T_{cp} = 16T_s$ is used in the CP-OFDM system, unless mentioned otherwise. Each component filter in the OFDM/OQAM system has maximum 12 taps.

Fig. 3 presents the reconstructed signal constellation in CP-OFDM systems. When there is no frequency dispersion, as in Fig. 3 (a,b), increased FFT size N decreases the distortion power. While for the purely frequency dispersive channel, as in Fig. 3 (c,d), increased FFT size significantly enlarges distortion. This confirms our analysis in Section 3.

Fig. 4 shows the signal reconstruction in OFDM/OQAM systems with EGF through doubly dispersive channel A. With the FFT size equals to 32, the one-tap FDE is far from perfect and therefore causes large distortion which is dominated by multipath fading. When N becomes large enough, the performance loss of one-tap FDE tends to be negligible while the distortion from frequency dispersion becomes large as $\frac{B_D}{F}$ increases. The system finally becomes frequency dispersion dominated where increasing the FFT size will only degrade the system performance.

Fig. 5 displays the frequency offset robustness of CP-OFDM and OFDM/OQAM systems with different FFT size over an ideal channel with only frequency offset added. These parallel curves have a similar slope which indicates that no matter in OFDM or OFDM/OQAM systems, the distortion caused by frequency synchronization imperfection is proportional to the normalized frequency offset with certain exponential order. In this figure, it is observed that the order is around 2, i.e. $\gamma_I^2 \propto (\frac{\Delta f}{F_s})^2$. With any FFT size, the OFDM/OQAM system always outperforms the CP-OFDM by about 1.5 dB.

4.3. Uncoded transmission

Fig. 6 illustrates the Bit Error Rate (BER) performance of uncoded transmission over doubly dispersive channels A and B with FFT size $N = 256$ and 4000 channel realizations. Cyclic prefix with length $T_{cp} = 16T_s$ are used in CP-OFDM and maximum 12 taps for each pulse shaping component filter are used in OFDM/OQAM systems. In channel A where all the multipath interference can be fully removed by cyclic prefix, CP-OFDM performs a little better than OFDM/OQAM systems (about 0.2 dB in high SNR region). However, when channel B is used, cyclic prefix alone cannot combat interference from "early" arrived paths, and therefore significantly degrades the performance of CP-OFDM. While OFDM/OQAM systems with different pulse shapes shows much stronger immunity and better performance. Besides, a considerable power and spectral

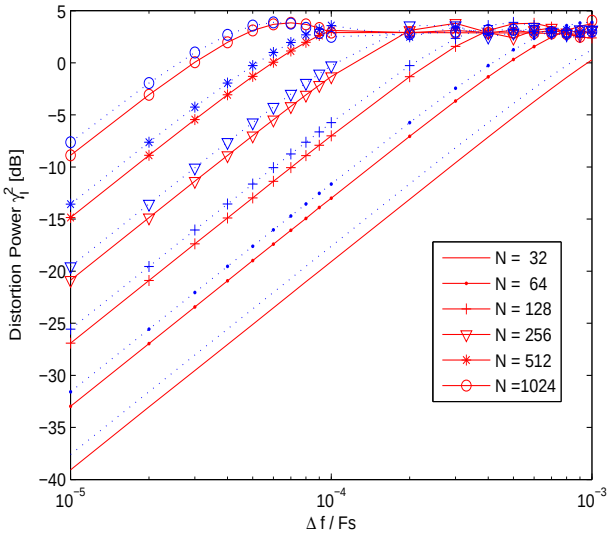

Figure 5. Frequency offset robustness for CP-OFDM (dotted line, $\frac{T_{cp}}{T} = 1/8$) and OFDM/OQAM (solid line, EGF $\alpha = 2$) systems.

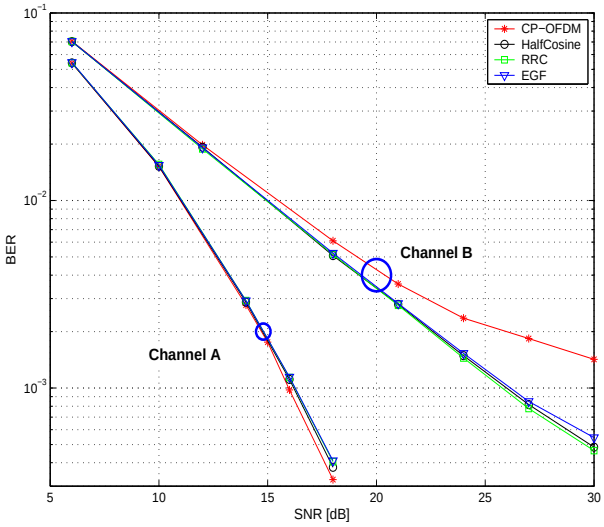

Figure 6. Uncoded BER versus SNR.

efficiency gain is achieved in OFDM/OQAM by not using cyclic prefix.

5. Conclusions

The signal reconstruction perfectness in both CP-OFDM and OFDM/OQAM systems over time and frequency dispersive channels has been analyzed and simulation results confirm relationship between FFT size and system interference characteristics, i.e., the interference is dominated either by delay spread or frequency spread. The simulation results showed that in interference dominated scenarios, it is necessary to carefully choose an appropriate transmission scheme with pulse shapes and FFT size to obtain desired performance. By using the same sampling frequency and sharing most of the common blocks, the integration of CP-OFDM and OFDM/OQAM becomes practical and straightforward.

References

[1] R. W. Chang, "Synthesis of Band-Limited Orthogonal Signals for Multi-carrier Data Transmission", *Bell. Syst. Tech. J.*, vol. 45, pp. 1775–1796, Dec. 1966.

[2] B. le Floch, M. Alard and C. Berrou, "Coded Orthogonal Frequency Division Multiplex," *Proceedings of the IEEE*, vol. 83, pp. 982–996, June 1995.

[3] P. Siohan, C. Siclet and N. Lacaille, "Analysis and design of OFDM/OQAM. systems based on filterbank theory", *IEEE Transactions on Signal Processing*, vol. 50, no. 5, pp. 1170–1183, May 2002.

[4] P. Jung, G. Wunder and C. S. Wang, "OQAM/IOTA Downlink Air Interface for UMTS HSDPA Evolution", *9th International OFDM-Workshop*, Hamburg, pp. 153–157, 2004.

[5] TIA Committee TR-8.5, "Wideband Air Interface Isotropic Orthogonal Transform Algorithm (IOTA) –Public Safety Wideband Data Standards Project – Digital Radio Technical Standards," TIA-902.BBAB (Physical Layer Specification, Mar. 2003) and TIA-902.BBAD (Radio Channel Coding (CHC) Specification, Aug. 2003) http://www.tiaonline.org/standards/.

[6] M. Bellec and P. Pirat, "OQAM performances and complexity," *IEEE P802.22 Wireless Regional Area Network (WRAN)*, Jan. 2006. http://www.ieee802.org/22/Meeting_documents/2006_Jan/22-06-0018-01-0000_OQAM_performances_and_complexity.ppt.

[7] B. Hirosaki, "An Orthogonally Multiplexed QAM System Using the Discrete Fourier Transform", *IEEE Transactions on Communications*, vol. 29, no. 7, pp. 982–989, Jul. 1981.

[8] L. Vangelista and N. Laurenti, "Efficient Implementations and Alternative Architectures for OFDM-OQAM Systems", *IEEE Transactions on Communications*, vol. 49, no. 4, pp. 664–675, Apr. 2001.

[9] J. Du and S. Signell, "Time Frequency Localization of Pulse Shaping Filters in OFDM/OQAM Systems", ICICS, Singapore, Dec. 2007, accepted.

[10] S. Signell and J. Huang, "A Matlab/Octave Simulation Workbench for Multi-Antenna Software Defined Radio", in Proc. of *24th Norchip Conference*, Linköping, Sweden, November 2006, pp. 145–148

[11] G. Lin, L. Lundheim and N. Holte, "On efficient equalization for OFDM/OQAM systems", *10th International OFDM-Workshop*, Hamburg, Germany, Aug. 2005.

[12] P. Siohan and C. Roche, "Cosine-Modulated Filterbanks Based on Extended Gaussian Function", *IEEE Transactions on Signal Processing*, vol. 48, no. 11, pp. 3052–3061, Nov. 2000.